A COMPARATIVE ANALYSIS OF FORECASTING METHODS FOR PHOTOVOLTAIC POWER AND ENERGY GENERATION WITH AND WITHOUT EXOGENOUS INPUTS

Anna Starosta, Komal Kaushik, Purav Jhaveri, Nina Munzke, Marc Hiller
Karlsruhe Institute of Technology,
Hermann-von-Helmholtz-Platz 1,
76344 Eggenstein-Leopoldshafen, Germany

ABSTRACT: With drive towards a green energy sector and significant cost reduction of photovoltaic (PV) technology, global PV capacity has increased multi folds in the last decade. PV power increases the variability of power supply due to the sun's changing position and weather volatility. Battery systems tackle these problems. For an optimized battery charging management, accurate PV energy forecasts are vital. The present work compares five 1-day-ahead PV power prediction models for a PV array of 8.64 kWp at KIT with 30° tilt and a 15° eastward orientation. The power prediction is used for intelligent battery charging management. The models are the offline persistence forecast (PF), an online forecast based on numerical weather prediction (NWP) and the machine-learning based offline Facebook prophet (FBP), support vector regression (SVR) and multilayer perceptron (MLP). According to the needs of intelligent battery charging management, the hourly PV energy forecast for the rest of the day is evaluated and compared for the different methods. The prediction methods are configurable for arbitrary inclinations and orientations. To the knowledge of the authors, FBP is compared for the first time to other models in the context of PV prediction. The results are evaluated for one year of data between March 2020 and February 2021. When comparing the performance of the models for different times of the day, SVR and MLP outperform the other models around noon, while the PF and most of the time NWP and FBP outperform the SVR and MLP in the morning and evening. When evaluating the models over one year, SVR outperforms the other model's power and energy prediction. At the same time, the other models have similar power prediction performance, but varying energy prediction performance. When evaluating the models over the meteorological seasons, there are striking differences of the models' performance. The SVR performs mostly best but is outperformed by the NWP in spring. At the same time, the NWP performs worst in winter. This is associated to reasons of spatial resolution of the NWP data. With the two best models SVR and MLP, it is shown that endogenous values generally suffice, while the partial outperformance of the NWP still motivates for a further investigation into the use of exogenous input.

Keywords: Battery storage and control, Evaluation, Photovoltaic, Software, PV Array, Solar Radiation

1 INTRODUCTION AND LITERATURE REVIEW

Photovoltaic (PV) power increases globally and has environmental and economic benefits. Its variable availability can be tackled by battery systems. Optimal battery charging management requires accurate energy forecasts [1]. The PV field of KIT Campus North with 102 PV arrays provides an attractive data basis for the research on power prediction. The power prediction is transformed into an energy forecast that serves the battery load management of a Li-ion battery system coupled to a PV array. The battery is charged so that it is full before sunset to prevent aging. Furthermore, the energy forecast is used to estimate the state of charge and state of health for batteries in advance [2]. Solar irradiation and resulting PV power can be predicted in several ways. While some methods use exogenous inputs such as the ambient temperature from a global forecasting system (GFS [3]) ("online" forecasts) [4, 5] others only use data collected on site ("offline" forecasts) [6, 7]. While the latter often use statistical methods in form of different time series analyses methods (persistence forecast (PF)), the former typically use numerical weather prediction (NWP) models. A combination of methods in order to merge advantages is common [8] but it has also been shown that univariate forecasting can achieve similar or even better accuracy compared to multivariate models [9, 10]. The PF as well as the NWP are based on physical equations that calculate the PV power output through considering the sun's position and radiation onto the tilted and specifically oriented PV array [11]. The difference between PF and NWP is the calculation of the global horizontal irradiance and using historical data in case of the PF [11] while using irradiance, albedo and ambient temperature from the GFS in case of the NWP [11, 12, 13].

In recent years, research has increasingly dealt with the application of machine learning (ML) in order to more accurately forecast the PV power and take advantage of patterns in historical data [14]. Popular and common approaches include support vector regression (SVR) and artificial neural networks (ANN), specifically deep learning methods [15]. SVR is the most extensively used ML algorithm in the field of PV power forecasting [9] because of its ability to find non-linear relationships and the small number of parameters to tune which is less likely to overfit the data [10]. Another approach is the time series model called Facebook prophet (FBP) which is faster than other statistical methods [16] and has shown promising results for PV forecasting [16]. In search of an optimal application of ML to PV forecasts, comparisons are regularly made [17, 18, 19] to find the best model, whereas the findings differ. To the knowledge of the authors, FBP is compared for the first time to other models in the context of PV prediction.

The present work introduces and compares five 1-day-ahead PV power prediction models for an example PV array, namely an online forecast based on NWP which uses exogenous and multivariate input and the offline, univariate PF, ML based FBP, SVR and multilayer perceptron (MLP) that only use endogenous input. The models' advantages and disadvantages are examined as well as their results compared and evaluated. The results are evaluated regarding the error metrics *MAE* and *RMSE* for specific times of the day, over the course of one year as well as for the meteorological seasons.

2 DATA INPUT

The 1 MWp PV field of KIT Campus North located at 49.1°N and 8.44°E provides an extensive dataset of several years of measured PV data at 1 second resolution. Here, a 8.64 kWp PV array with 30° tilt and a 15° eastward orientation has been chosen to train and test the different models. The considered meteorological seasons are divided into spring (March to May), summer (June to August), autumn (September to November) and winter (December to February). The time range of spring 2020 till winter 2020/2021 is considered.

3 FUNDAMENTALS

3.1 Physical Principles

The PV power is calculated using the direct irradiance I_{dir} excluding the incident angle losses contained in the incident angle modifier IAM_{b} [20], the diffuse irradiance I_{dif} [21, 22] and the ground diffuse (reflected) irradiance I_{ref} [13] in the plane of the PV array, as in

$$P_{\mathrm{PV}} = \eta_{\mathrm{PV}} \cdot A_{\mathrm{PV}} \cdot (IAM_{\mathrm{b}} \cdot I_{\mathrm{dir}} + I_{\mathrm{dif}} + I_{\mathrm{ref}}) \qquad (1)$$

where η_{PV} denotes the efficiency of the PV array and A_{PV} denotes the PV panel size. A more detailed overview can be found in [23]. The global irradiance from which the direct and diffuse irradiance is derived as well as other parameters are obtained depending on the offline or online approach and are therefore explained in subsections 4.1 and 4.2 respectively.

3.2 Machine Learning and Time-Series Forecasting

In Machine-learning (ML), PV power time series forecasting can be viewed as a supervised regression problem [24]. In this work, only the past values of the time series as endogenous values are used. So called direct multi-step ahead methods are applied.

Deep Learning is a subfield of ML and uses artificial neural networks (ANNs) as its basic structure. The ANN comprises an input and output layer as well as a variable number of hidden layers. The layers consist of neurons, also called nodes or units. The most fundamental form of an ANN is a feed-forward network where the information flow happens in a forward direction [25].

An essential part of building an ML model is the training of the model minimizing a loss function while using training data and afterwards testing the model on unseen testing data.

3.3 Energy Forecast

The energy forecast uses the forecasted power values $P(t)$. The expected energy $E(t_i)$ for the rest of the day at time point t_i corresponds with the integration of the power $P(t)$ from t_i until the end of the day T, as in:

$$E(t_{\mathrm{i}}) = \int_{t_{\mathrm{i}}}^{T} P(t)\, dt \qquad (2)$$

4 FORECASTING MODELS

4.1 Persistence Forecast

The Persistence Forecast (PF) model is an offline model that only uses endogenous parameters. It is based on the physical equations explained in section 3.1 and assumes persisting weather conditions for a specific time horizon [1, 4]. In this work, a day-ahead prediction P_{PF} is made by scaling the clear-sky power curve of the predicted day $P_{\mathrm{CS,T}}$, as described in Equation (3)

$$P_{\mathrm{PF}} = k_{\mathrm{PF}} \cdot P_{\mathrm{CS,T}} \qquad (3)$$

with the scaling factor k_{PF} based on the generated PV energy of the previous day $E_{\mathrm{Real,T-1}}$ and the PV energy $E_{\mathrm{CS,T-1}}$ that would have been generated on a clear-sky day, as described in Equation (4)

$$k_{\mathrm{PF}} = \frac{E_{\mathrm{Real,T-1}}}{E_{\mathrm{CS,T-1}}} \qquad (4)$$

The clear-sky power curve $P_{\mathrm{CS,T}}$ is calculated using Equation (1). As the PF model only has access to offline parameters, the global horizontal irradiance is calculated using the approaches in [26, 27] as further explained in [11]. The albedo is calculated using the equations in [13, 21].

Advantages of the PF model are its independency on exogenous variables or larger datasets, its simplicity, robustness and short computing times of less than one minute. Disadvantage is its reduced accuracy for the 1-day-ahead prediction.

4.2 Numerical Weather Prediction

The Numerical Weather Prediction (NWP) model is an online forecasting model that uses the exogenous inputs ambient temperature, global horizontal irradiance and albedo coefficient. The NWP is based on the Global Forecasting System (GFS) provided open-source by [3]. Similar to the PF, the calculation of PV power is based on Equation (1), while the PV efficiency η_{PV} is calculated depending on the GFS's predicted ambient temperature [28]. The global horizontal irradiance and the albedo coefficient are taken from the GFS's data and are handled using the equations in [21, 26]. The diffuse irradiance comprises the differentiation between a twilight zone before sunrise and after sunset using the equations in [21, 22] and times of direct sunlight using the equations in [21, 29].

The NWP data is updated every 6 h and its data is available in a 1-hour temporal resolution and a 0.25° spatial resolution. In this work, the midnight update is used for the 24 h day-ahead prediction.

Advantages of the NWP are the possibility to use a vast range of predicted parameters. Disadvantages are its need for an online connection, the large GFS files that need to be downloaded and processed and therefore increased computing times of one to two hours for this work's NWP model.

4.3 Facebook Prophet Algorithm

The Facebook Prophet Algorithm (FBP) is a univariate time series forecasting tool and uses only offline time series PV power data as an input. FBP is based on an additive regression model stated as described in [16]

$$y(t) = g(t) + s(t) + h(t) + e(t) \qquad (5)$$

Table I: Choice of FBP parameters

Parameter	Value
growth	linear
seasonality mode	multiplicative
change point prior scale	10
fourier order	15

with the time-dependent functions for trends *g(t)*, periodic changes *s(t)*, irregular predictable occasions *h(t)* and independent identically distributed noise *e(t)* (see Equation (5)). Advantages of the FBP are, that the statistical method is relatively simple and robust to outliers, missing values and sudden changes. Disadvantages are its dependency on larger datasets [16]. In this work, the parameters were tuned using manual tuning, also known as exhaustive search, on training data. An input of the prior 3 months' data showed to be optimal. This work's FBP model needs 2.5 minutes to load the input data and about 40 seconds to calculate. The optimized parameters are as shown in Table I.

4.4 Support Vector Regression

Support Vector Regression (SVR) is a supervised ML technique for regression analysis. Here, only offline PV power data is used as input. SVR is able to handle non-linear data using a kernel function, a set of mathematical functions, which model the input data into a higher dimensional space. Goal is to find a hyperplane (decision boundary) in an *n*-dimensional space that classifies the data points. SVRs are based on so called maximum-margin classifiers as the distance of the data points closest to the hyperplanes (support vector) is maximized and therefore the optimal orientation and location of the hyperplane is achieved. At the core of the technique, the distance between the data points outside a permitted marginal error ε, so called slack variables ξ and ξ*, are minimized, as in [30]

$$\min\left(\frac{1}{2}\|w\|^2 + C\sum_{i=1}^{n}\left|\xi_{\mathrm{i}}\right|\right) \qquad (6)$$
$$s.t.\,|y_{\mathrm{i}} - w_{\mathrm{i}}x_{\mathrm{i}}| \le \varepsilon + |\xi_{\mathrm{i}}|$$

with the target *y,* the features *x,* the weight *w* and the tunable penalty of error term *C* (see Equation (6)). The parameters were tuned using random search optimization with the search space 'rbf'-kernel, *C* = [0.1, 0.5, 1, 10, 16], the tube-defining ε = [0.01, 0.1, 1], the kernel coefficient γ = [0.1, 0.01, 1, 10, 100, 1000]. The parameters were tuned on the basis of 1.3 years and 11 days input data predicting according days in winter and summer. The optimized parameters are shown in Table II. Furthermore, a training data set of the prior 6 months of PV power data of the predicted day showed to be optimal. SVR is the most extensively used ML algorithm in the field of PV power forecasting [9] because of its ability to find non-linear relationships and the small number of parameters that have to be tuned. Therefore, it is less likely to overfit the data [10]. Furthermore, this work's SVR needs about 5 minutes

Table II: Choice of SVR parameters

Parameter	Value
kernel	*rbf*
C	16
γ	0.01
ε	0.1

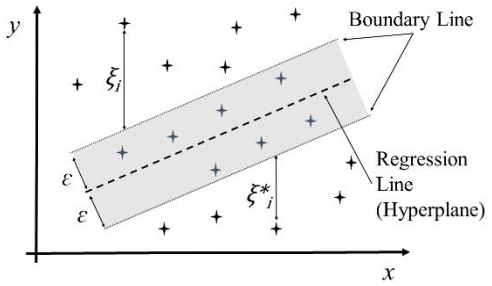

Figure 1: Basic principle of the SVR model. All errors outside an error tolerance ε are optimized towards the regression line.

for processing the input data while the algorithm itself needs about 12 seconds. A disadvantage is, that it depends on larger datasets.

4.5 Multilayer Perceptron

Multilayer Perceptrons (MLPs) are feed-forward ANNs with one or more hidden layers of non-linearly-activating nodes. The hidden layers consist of so called perceptrons which are multiple input single output units processing binary data *z* with a chosen non-linear activation function *f*. The unit input *x* is multiplied by weights *w* which are adjusted during the training phase in order to minimize the output error. For each unit, the basic principle looks as follows, where a bias is added for a non-zero output as described in Equation (7) [31]

$$z = \begin{cases} 0, & \sum_{i=1}^{m} w_i x_i + bias < 0 \\ 1, & \sum_{i=1}^{m} w_i x_i + bias \ge 0 \end{cases} \qquad (7)$$

$$\hat{y} = f(z)$$

with $\hat{y}$ being the output of the unit. MLPs learn via backpropagation in order to adjust the unit weights for minimizing the error of the overall output calculated as described in Equation (8)

$$\varepsilon(n) = \frac{1}{2}\sum_{j} e_j^2(n) \qquad (8)$$

The number of hidden units and layers has to be optimized and tuned [32]. Figure 2 shows the basic operating principle of the MLP model for the 1-day-ahead PV power prediction. The input data has an hourly resolution.

ANNs are popular deep learning algorithms for PV power forecasting that are currently further investigated in literature [6, 32]. At the same time it is difficult to determine the high number of hyper-parameters [33] and the MLP depends on larger datasets. The MLP used in this work needs about 5 minutes to load the input data and about 4 minutes to apply the MLP algorithm. After a first manual tuning, the hyper-parameters were further optimized using random search optimization. The parameters were tuned on the basis of 1.3 years and 11 days input data predicting according days in winter and summer. The search space includes 3 input neurons, 2 hidden layers, 2 to 40 neurons in the hidden layers, "adam" optimizer and the "relu" and "softplus" activation functions. The optimized hyper-parameters are found in Table III. Furthermore, a training data set of the prior 6 months of PV power data of the predicted day showed to be optimal.

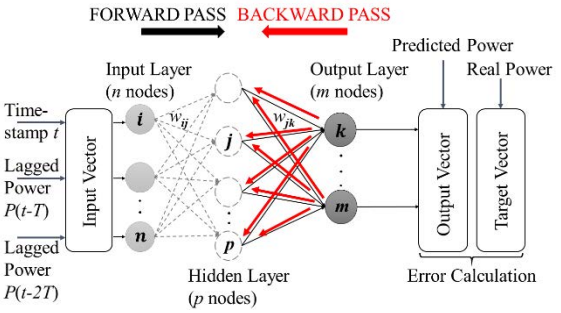

Figure 2: Basic operating principle of the MLP model. The timestamp *t* and lagged power from 1 and 2 days prior (*P(t-T)* and *P(t-2T)*) are used as inputs for the input layer. The values are processed via the hidden layers and the output error is calculated. The weights are tuned via backpropagation [31].

Table III: Choice of MLP parameters

Parameter	Value
optimizer	*adam*
neurons in input layer	3
neurons in hidden layer 1	18
neurons in hidden layer 2	26
activation functions	*relu, softplus*
neurons in output layer	1
epochs	11688
batch size	10000

5 DATA PRE- AND POST-PROCESSING

FBP processes the data automatically while SVR and MLP need feature engineering [24]. Date time features including hours of the day as well as the power value of a previous time step, called lag feature, are chosen. Furthermore, the data is transformed via standardization and normalization. After prediction, the results are inversely transformed again. For SVR, the lag combination of power *P(t-T)* is chosen, where *t-T* denotes the value one-day prior. For MLP, the combination of *P(t-T)* and *P(t-2T)* performed slightly better. The input data has a 1-hour resolution.

Prediction data outside the sunrise and sunset times (at nighttime) were set to zero so that the models are only compared for relevant times of PV power generation.

6 EVALUATION METRICS

6.1 Mean Absolute Error

The mean absolute error *MAE* shows the mean absolute deviation of the prediction values *y* from the actual values *x* for each time point *t* and the time range *n*. The *MAE* is less sensitive towards outliers.

$$MAE = \frac{\sum_{t=1}^{n} |y(t) - x(t)|}{n} \quad (9)$$

6.2 Root Mean Square Error

The root mean square error *RMSE* is more sensitive towards outliers as it regards the square of the deviations, as in:

$$RMSE = \sqrt{\frac{\sum_{t=1}^{n} (y(t) - x(t))^2}{n}} \quad (10)$$

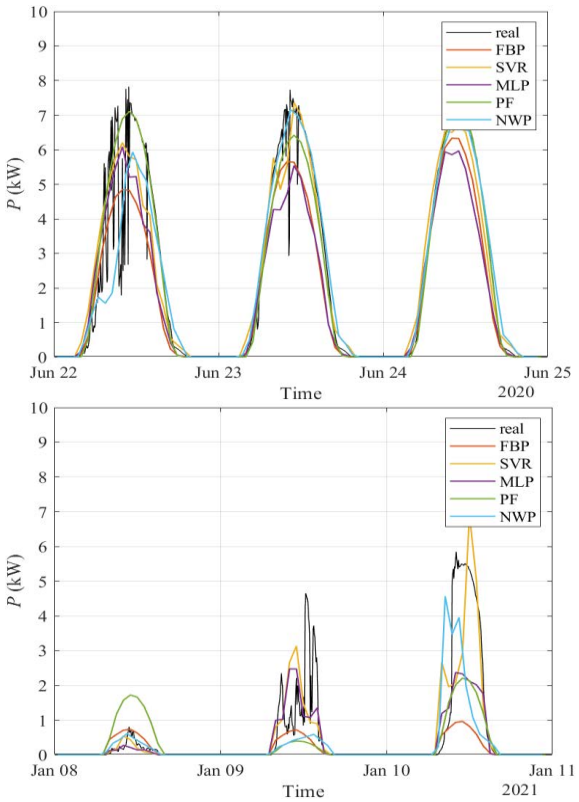

Figure 3: Exemplary measured and predicted power on three days in summer 2020 (upper panel) and winter 2021 (lower panel) comparing the FBP, SVR, MLP, PF and NWP model.

7 RESULTS

7.1 Real and Predicted Power in Winter and Summer

Before comparing the models via error metrics, example days in summer and winter are shown to give a first impression on the different models and their differing ability to react to weather patterns.

Figure 3 (upper panel) shows three exemplary days in summer 2020 with the real power in kW as the black curve and the different models in colors. The fluctuating real power curves on June 22nd and June 23rd indicate moving clouds, otherwise there are long time periods of clear-sky conditions with a peak power of 7 kW due to the PV array's tilt and orientation. Comparing the daily changing performance of models, the FBP model adapts too slowly to the almost clear-sky conditions, ranging between 4.7 kW on June 22nd and 6.5 kW on June 24th. The SVR model performs well and only underestimates the power of June 22nd and June 24th by about 0.5 kW to temporarily 1.5 kW. The MLP model underestimates all three days by 1.5 to 2 kW. The PF model predicts the power well as there are little weather changes and nearly persisting weather conditions. The NWP model also performs well and only underestimates the power of June 22nd by 1.2 kW.

Figure 3 (lower panel) shows three exemplary days in winter 2020/2021. Here, the real power fluctuates highly. The first exemplary day, January 8th, shows the typical power pattern for a day with a thick cloud layer with a maximum PV power of 0.8 kW. January 9th shows changing clouds with an occasional increase in solar irradiance with a PV power up to 4.5 kW. January 10th

shows even more solar irradiance with an initial lack of light in the morning and early noon and a peak power of 6 kW. Here, the reduced peak power of about 6 kW is obvious due to winter time. For these three days, the models' adaptability to weather changes is required. The FBP model again adapts too slowly and underestimates the power of January 9th and January 10th by up to 4.5 kW. The SVR model predicts the power well. The MLP model predicts the power well, too, but underestimates the power on January 10th by far with a difference of 4.5 kW. The PF model does not cope with the weather changes well as the assumption of persisting weather conditions of the previous day do not hold true. Therefore, the PF model overestimates the power by 0.8 kW (January 8th) and underestimates the power by 4 kW (January 9th) and by 3.4 kW (January 10th). The NWP model also mostly underestimates the power by an average of 2.4 kW but performs better than the PF model.

7.2 Real and Predicted Energy in Winter and Summer

According to Equation (2), the energy is calculated for each power curve. As a result, Figure 4 (upper panel) shows the energy prediction on three exemplary days in summer. Again, there are significant differences between the models. The SVR and PF predict the energy similarly well under- or overestimating the energy at maximum by 5 kWh. The MLP and FBP perform continuously bad, underestimating the generated energy by up to 15 kWh.

Figure 4 (lower panel) shows the energy prediction on three exemplary days in winter. The most accurate energy prediction is performed by the SVR model under- or overestimating the energy at maximum by 1 kWh. The FBP and PF perform worst, under- or overestimating the energy up to 10 kWh. Most notably, the PF does not adapt due to the high differences in weather conditions between each day.

Both the power and energy forecasts on the exemplary days give the motivation to find which model works best under what circumstances.

7.3 Comparison of PF, NWP, FBP, SVR and MLP

The model comparison comprises two approaches. First, the errors of the power prediction is calculated from spring 2020 till winter 2020/2021 over one year for the time of the day (see Equations (9) and (10)).

Figure 5 shows the corresponding model errors over the day. Due to the lack of normalization, it is not possible to compare a model with itself for different times of the day. The focus lies on the comparison of the different models with each other. It stands out that there are differences between the morning, noon and evening times.

Figure 5 (upper panel) shows the *MAE* of the power predictions' error over the day. During noon time between 8 am and 3 pm (UTC), SVR performs best with a *MAE* of around 1 kW, followed by the MLP, NWP and lastly the FBP and PF models with a MAE of up to 1.75 kW. Strikingly, the performance of the models turns around at morning and evening times between about 4 am to 8 am (UTC) and 3 pm to 8 pm (UTC). Here, the PF and NWP model work best in the morning and the PF model in the evening, which indicates that a prediction based on physical equations has an advantage calculating sunrise and sunset times with more accuracy than machine-learning models can, although the FBP model is similarly good at detecting the regularities. The worst performance is observed for the MLP model with a *MAE* of up to 0.5 kW.

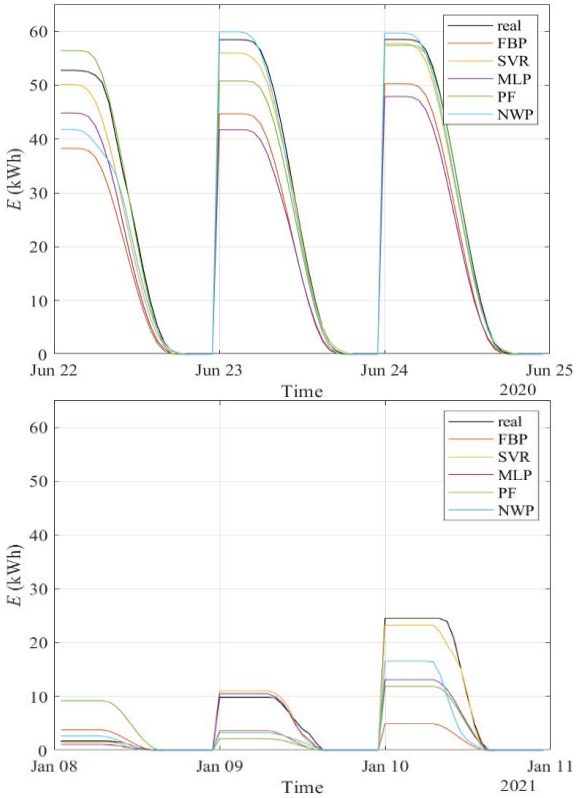

Figure 4: Exemplary measured and predicted energy for the remaining day on three days in summer 2020 (upper panel) and winter 2021 (lower panel) comparing the FBP, SVR, MLP, PF and NWP.

Table IV: Errors over one year for each model

	PF	NWP	FBP	SVR	MLP
MAE (kW)	0.51	0.47	0.55	0.42	0.51
RMSE (kW)	1.15	1.05	1.12	0.88	1.01
MAE (kWh)	4.83	3.65	4.89	1.81	3.21
RMSE (kWh)	9.24	7	8.49	3.8	5.98

Figure 5 (lower panel) shows the *RMSE* of the power predictions' error over the day. The course is similar to that of the *MAE* with the SVR model performing best during the day with a *RMSE* up to 1.5 kW. During noon time, the PF model shows to be more prone to outliers and performs slightly worse than the FBP. Similarly, the NWP is more prone to outliers than the MLP. The difference between the *RMSE* of the MLP and NWP is about 0.1 kW higher than that of the *MAE*. Still, there are high differences in the models at mornings and evenings, where the PF and NWP models based on physical equations and the FBP model with its ability to detect patterns perform better than the SVR and MLP models. Here, the difference in *RMSE* is more noticeable in the morning than the evening. The bad performance of the MLP increases from a *MAE* of about 0.5 kW to a *RMSE* of about 0.8 kW and shows to be derived especially from outliers.

In a second approach, the errors (see Equations (9) and (10)) of the power and energy are calculated over time ranges, namely the different meteorological seasons and one year.

Table IV shows the errors of power and energy forecasts for the entire year under consideration. It is obvious that the SVR model outperforms all other models irrespective of the power or energy prediction with a *MAE*

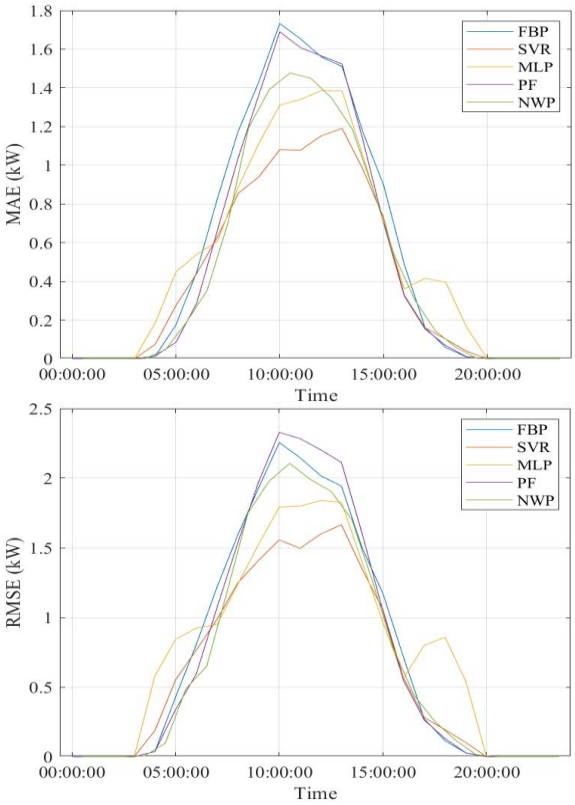

Figure 5: Error of the power prediction calculated over one year (spring 2020 – winter 2020/2021) for specific times of the day.

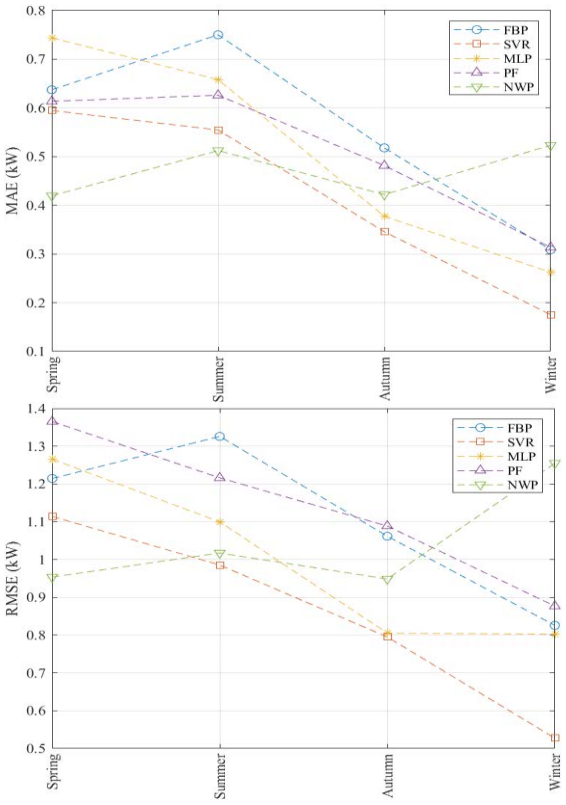

Figure 6: Error of the power prediction calculated for different seasons, namely spring, summer, autumn and winter 2020/2021.

of 0.42 kW and 3.8 kWh and a *RMSE* of 0.88 kW and 3.8 kWh. Concerning the power prediction, PF, NWP, FBP and MLP perform in a similar range with a *MAE* of about 0.5 kW. The energy prediction shows higher differences in performance, where the MLP model performs second best, followed by the NWP, FBP and lastly PF model with a *MAE* of 4.83 kWh and *RMSE* of 9.24 kWh.

In order to evaluate the accuracy of the models in more detail, the *MAE* and *RMSE* are also calculated for the different meteorological seasons.

Figure 6 (upper panel) shows the *MAE* of the power prediction over the different seasons. It is striking that the performance of the models can differ a lot depending on the time of the year. While the NWP model performs best in spring and summer with a *MAE* of 0.42 kW and 0.5 kW respectively, it performs worst in winter with about 0.52 kW. A similar contrast is observed for the MLP model which performs worst and second worst in spring and summer with 0.74 kW and 0.66 kW respectively, while it performs second best in autumn and winter with 0.4 and 0.28 kW respectively. The bad performance of the MLP in spring and summer indicates that the high errors observed in the morning and evening in Figure 5 are mostly to be related to the spring and summer time. In general, the PF and FBP model perform rather bad, while the PF's *MAE* is slightly better than that of the FBP. The SVR model performs overall well and best for autumn and winter with 0.35 and 0.18 kW respectively.

Figure 6 (lower panel) shows the *RMSE* of the power prediction over the different seasons. The difference of the course of the *RMSE* to the one of the *MAE* are to be found in a slightly better performance of the MLP and SVR with a *RMSE* between 0.1 kW and 0.35 kW lower than the respectively worst performing model, while the PF model performs slightly worse now representing the worst performing model in spring, autumn and winter with 1.36, 1.12 and 0.89 kW respectively. This indicates, that MLP and SVR are less prone to outliers, whereas PF is. The NWP model shows a decline in performance in winter from a difference of 0.2 kW *MAE* to 0.35 kW *RMSE* to the next best model which indicates that the NWP is more prone to outliers especially in winter. It is to be assumed that the partly bad performance of the NWP is related to spatial differences in the accuracy of the GFS data. Overall, the SVR model generally performs best again with a *RMSE* of 1.11, 1.0, 0.8 and 0.53 kW in spring, summer, autumn and winter respectively, with only the NWP model performing better in spring with 0.96 kW.

Figure 7 (upper panel) shows the *MAE* of the energy prediction over the different seasons. Similar to the error values over one year, the seasonal evaluation of the energy prediction shows stronger differences between the models. Especially the PF model worsens compared to the FBP model with a *MAE* of 5.8 kWh, 4.7 kWh and 3.5 kWh in spring, autumn and winter respectively and only outperforms the FBP model in summer with a *MAE* of 5.6 kWh compared to 6.4 kWh for the FBP. The MLP and SVR model clearly improve and the SVR model strengthens its superiority with a *MAE* of 1.6 kWh, 1.1 kWh and 0.85 kWh in summer, autumn and winter respectively, except for spring time, where the NWP still performs best with 2.85 kWh compared to 3.6 kWh for the SVR. The SVR's improvement is most apparent in summer and autumn.

Figure 7 (lower panel) shows the *RMSE* of the energy prediction over the different seasons. The development and stronger clarity of model differences is similar to that of the *MAE* where again the PF model shows to deal worse

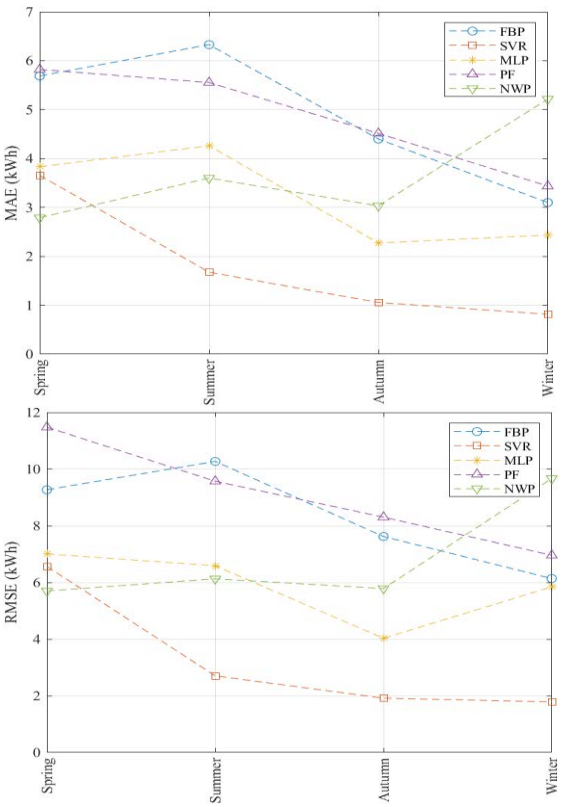

Figure 7: Error of the energy prediction calculated for different seasons, namely spring, summer, autumn and winter 2020/2021.

with outliers with a *RMSE* of 11.5 kWh, 9 kWh and 7 kWh in spring, autumn and winter respectively, where only the FBP model is worse in summer with 10.2 kWh, while the SVR does not seem to be much affected by outliers with a *RMSE* of 6.5 kWh, 2.8 kWh, 2 kWh and 1.95 kWh in spring, summer, autumn and winter respectively, only outperformed by the NWP model in spring with a *RMSE* of 5.8 kWh.

8 CONCLUSION AND OUTLOOK

The present work introduces different 1-day-ahead PV power prediction models for a PV array of 8.64 kWp at KIT with a tilt of 30° and an eastward orientation of 15°. The considered models namely the persistence forecast (PF), numerical weather prediction (NWP), Facebook prophet algorithm (FBP), support vector regression (SVR) and multilayer perceptron (MLP) are compared.

There is a striking difference of performance offered by the above-mentioned models during noon, morning and evening. The SVR and MLP models outperform the other models at noon, while the PF, (most of the time) NWP and FBP outperform the SVR and MLP at morning and evening times.

An evaluation over one year shows the SVR to be outstanding, while the model could not outperform the NWP model in spring. Other than the SVR, all other models have similar power prediction performance and only the energy prediction shows differences. The MLP performs second best, followed by NWP, FBP and lastly PF.

It is shown that an evaluation of the models' accuracy for the meteorological seasons throughout a considered year from spring 2020 till winter 2020/2021 shows significant differences of the models' performance depending on the time of the year. The strong differences in the NWP model's accuracy indicate a spatial influence of the GFS data and motivate for a differentiated use of the model depending on the location.

It is expected that with further tuning of the MLP's hyper-parameters, it's performance during morning and evening could be increased.

With the two overall most accurate models SVR and MLP, it is shown that endogenous values generally suffice, while the partial outperformance of the NWP still motivates for a further investigation into the use of exogenous input.

Concluding, it makes sense to look at the differences in times of the day and seasons, as different models perform differently well for different times of the day and year. The advantages of the different models can therefore temporally be combined into according hybrid models.

As the PV predictions are used for battery charging management, further investigations into intraday-forecasts are necessary. An according PF and NWP model is already available at the institute and will be further evaluated.

This will be part of future work.

9 REFERENCES

[1] J. Barry und J. Thomas, „Online and Offline PV Power Forecasts for Optimal Control of Storage Systems," *33rd European Photovoltaic Solar Energy Conference Classhighlight SpanExhibitions,* pp. 2729-2732, November 2017.

[2] B. Verma und N. Munzke, „Performance of In-house Li-ion Battery Storage Systems Based on Various Strategies," *EU PVSec Proceedings,* 2018.

[3] NOAA, „NCEP Products Inventory: Global Products," National Weather Service, [Online]. Available: https://www.nco ncep noaa.gov/pmb/products/gfs/. [Zugriff am 09 09 2021].

[4] R. H. Inman, H. T. C. Pedro und C. F. M. Coimbra, „Solar Forecasting Methods for Renewable Energy Integration," *Progress in Energy and Combustion Science,* pp. 535-576, 2013.

[5] E. Lorenz, J. Kühnert, D. Heinemann, K. P. Nielsen, J. Remund und S. C. Müller, „Comparison of Global Horizontal Irradiance Forecasts Based on Numerical Weather Prediction Models with Different Spatio-temporal Resolutions," *Progress in Photovoltaics: Research and Applications,* pp. 1626-1640, 2016.

[6] H. T. C. Pedro und C. F. M. Coimbra, „Assessment of Forecasting Techniques for Solar Power Production Without Exogenous Inputs," *Solar Energy,* pp. 2017-2028, 2012.

[7] V. Badescu, „3D Isotropic Approximation for Solar Diffuse Irradiance on Tilted Surfaces," *Renewable Energy,* pp. 221-233, 2002.

[8] J. Antonanzas, N. Osorio, R. Escobar, R. Urraca, F. J. Martinez-de-Pison und F. Antonanzas-Torres, „Review of Photovoltaic Power Forecasting," *Solar Energy,* pp. 78-111, 2016.

[9] M. Rana, I. Koprinska und V. Agelidis, „2D-interval Forecasts for Solar Power Production," *Solar Energy,* pp. 191-203, 2015.

[10] M. Rana und A. Rahman, „Multiple Steps Ahead Solar Photovoltaic Power Forecasting Based on Univariate Machine Learning Models and Data Re-sampling," *Sustainable Energy, Grids and Networks,* p. 100286, March 2020.

[11] J. A. Thomas, „Optimisation Method for the Clear Sky PV Forecast Using Power Records from Arbitrarily Oriented Panels," in *7th International Conference on Renewable Energy Research and Applications (ICRERA)*, Paris, 2018.

[12] D. T. Reindl, W. A. Beckman und J. A. Duffie, „Diffuse Fraction Correlations," *Solar Energy,* pp. 1-7, 1990.

[13] P. G. Loutzenhiser, H. Manz, C. Felsmann, P. A. Strachan, T. Frank und G. M. Maxwell, „Empirical Validation of Models to Compute Solar Irradiance on Inclined Surfaces for Building Energy Simulation," *Solar Energy,* pp. 254-267, 2007.

[14] A. Mellit, A. Massi Pavan, E. Ogliari, S. Leva und V. Lughi, „Advanced Methods for Photovoltaic Output Power Forecasting: A Review," *Applied Sciences,* p. 487, 2020.

[15] Y. LeCun, Y. Bengio und G. Hinton, „Deep Learning," *Nature,* pp. 436-444, 2015.

[16] M. M. Hasan Shawon, S. Akter, M. K. Islam, S. Ahmed und M. M. Rahman, „Forecasting PV Panel Output Using Prophet Time Series Machine Learning Model," *2020 IEEE Region 10 Conference (Tencon),* 2020.

[17] H. Long, Z. Zhang und Y. Su, „Analysis of Daily Solar Power Prediction with Data-driven Approaches," *Applied Energy,* pp. 29-37, 2014.

[18] M. Abuella und B. Chowdhury, „Solar Power Forecasting Using Support Vector Regression," in *arXiv preprint*, 2017.

[19] S. Theocharides, G. Makrides, G. E. Georghiou und A. Kyprianou, „Machine Learning Algorithms for Photovoltaic System Power Output Prediction," in *2018 IEEE International Energy Conference (ENERGYCON)*, 2018.

[20] W. De Soto, S. A. Klein und W. A. Beckman, „Improvement and Validation of a Model for Photovoltaic Array Performance," *Solar Energy,* pp. 78-88, 2006.

[21] J. E. Hay, „Calculating Solar Radiation for Inclined Surfaces: Practical Approaches," *Renewable Energy,* pp. 373-380, 1993.

[22] B. Y. H. Liu und R. C. Jordan, „The Interrelationship and Characteristic Distribution of Direct, Diffuse and Total Solar Radiation," *Solar Energy,* pp. 1-9, 1960.

[23] W. Holmgren, C. Hansen und M. Mikofski, „pvlib Python: A Python Package for Modeling Solar Energy Systems," *Journal of Open Source Software,* p. 884, 2018.

[24] J. Brownlee, Introduction to Time Series Forecasting with Python: How to Prepare Data and Develop Models to Predict the Future, Machine Learning Mastery, 2017.

[25] I. Goodfellow, Y. Bengio und A. Courville, Deep Learning, MIT Press, 2016.

[26] R. Perez, P. Ineichen, K. Moore, M. Kmiecik, C. Chain, R. George und F. Vignola, „A New Operational Model for Satellite-derived Irradiances: Description and Validation," *Solar Energy,* pp. 307-317, 2002.

[27] P. Ineichen und R. Perez, „A New Airmass Independent Formulation for the Linke Turbidity Coefficient," *Solar Energy,* pp. 151-157, 2002.

[28] E. Skoplaki und J. A. Palyvos, „On the Temperature Dependence of Photovoltaic Module Electric Performance: A Review of Efficiency/Power Correlations," *Solar Energy,* pp. 614-624, 2009.

[29] D. T. Reindl, W. A. Beckman und J. A. Duffie, „Diffuse Fraction Correlations," *Solar Energy,* pp. 1-7, 1990.

[30] M. Awad und R. Khanna, „Efficient Learning Machines: Theories, Concepts and Applications for Engineers and System Designers," *Springer nature,* p. 268, 2015.

[31] K.-L. Du und M. N. S. Swamy, „Multilayer Perceptrons: Architecture and Error Backpropagation," *Neural Networks and Statistical Learning,* pp. 97-141, 2019.

[32] D. L. Chester, „Why Two Hidden Layers are Better Than One," *Proceedings IJCNN,* pp. 265-268, 1990.

[33] F. Hutter, H. Hoos und K. Leyton-Brown, „An Efficient Approach for Assessing Hyperparameter Importance," in *International Conference on Machine Learning*, 2014.

[34] M. Rana, I. Koprinska und V. Agelidis, „Univariate and Multivariate Methods for Very Short-term Solar Photovoltaic Power Forecasting," *Energy Conversion and Management,* pp. 380-390, 1 August 2016.

[35] A. Mellit und A. M. Pavan, „A 24-hour Forecast of Solar Irradiance Using Artificial Neural Network: Application for Performance Prediction of a Grid-connected PV plant at Trieste, Italy," *Solar Energy,* pp. 807-821, 2010.

[36] S. J. Taylor und B. Letham, „Forecasting at Scale," *Peer Preprints,* 2017.